Properties of $Fe_{73.5-x}Si_{13.5}B_9Cu_1Nb_3Mn_x$ Alloys by Means of Mössbauer Spectroscopy

R. Brzozowski[a], M. Wasiak[b], J. Balcerski[c], P. Sovák[c]
and M. Moneta[a,*]

[a]Wydział Fizyki i Informatyki Stosowanej, Uniwersytet Łódzki
Pomorska 149, 90-236 Łódź, Poland

[b]Wydział Chemii, Uniwersytet Łódzki, Pomorska 163, 90-236 Łódź, Poland

[c]Univ. P.J. Šafárika, Prirod. Fakulta, Park Angelinum 9, 04-101 Košice, Slovakia

$Fe_{73.5-x}Si_{13.5}B_9Cu_1Nb_3Mn_x$ ($x = 1, 3 \div 15$) amorphous alloys were studied by means of Mössbauer spectroscopy, as-quenched and after annealing. The basic alloys show stronger magnetic ordering for small values of x, than for larger x. The initially amorphous phase and the final nanocrystalline structure were determined with X-ray diffraction. The alloys were shown, by scanning calorimetry, to suffer different phase transformations, when heated.

PACS numbers: 75.50.Bb, 75.50.Ww, 75.60.Ej

1. Introduction

Iron-based alloys, like $Fe_{73.5}Si_{13.5}B_9Cu_1Nb_3$ finemet, consist primarily of amorphous-magnetic phase. After appropriate thermal treatment the alloys are transformed to the mixture phase where iron-silicate nano-crystals are embedded in an amorphous residual matrix [1, 2]. In previous papers the temperature dependence of structure and magnetic properties of $Fe_{73.5-x}Si_{13.5}B_9Cu_1Nb_3Mn_{x=0}$ were analysed [3, 4]. The Mössbauer spectroscopy (MS) shows multiple narrow lines, which represent structurally different crystallographic sites assigned to the iron-silicate grains, superimposed on a broadened feature ascribed to the residual amorphous phase [5–8].

2. Experiment

The 30 μm amorphous ribbons of $Fe_{73.5-x}Si_{13.5}B_9Cu_1Nb_3Mn_x$ ($x = 1, 3 \div 15$) were quenched from master alloys by a melt-spinning technique.

---

*corresponding author; e-mail: marek_moneta@uni.lodz.pl

In the MS transmission experiments the ^{57}Co:Rh source with activity of about 100 mCi was used. The numerical analysis of the Mössbauer spectra was performed with RECOIL packet. The MS measurements were supplemented by X-ray diffraction (XRD) patterns measured with Philips PW 1830 Cu K_α generator, differential scanning calorimetry (DSC) with Setaram TG DSC-111 and electron diffraction spectroscopy (EDX) with Link300 ISIS Oxford Instruments.

3. Results and discussion

From the thermal study of the original finemet ($x = 0$) [2–4] two fractions: amorphous and crystalline were identified and characteristic parameters were determined. The amorphous structure of the alloys can be demonstrated by absence of any XRD lines up to $T_{\text{FeSi-cryst}} \approx 480°$C. It is known that the heated sample remains ferromagnetic and amorphous up to the Curie temperature $T_{\text{C}}^{\text{am}} = 328°$C. It remains paramagnetic up to crystallisation temperature $T_{\text{cryst}} = 480°$C (XRD) [4] or 513°C (vibrating sample magnetometer, VSM) [2] or 483°C (MS), 527°C (DSC), 532°C (VSM) [5], when magnetisation appears again as a consequence of crystallisation to five Fe–Si crystal-ferromagnetic structures [6]. The crystalline grain size starts from $d \approx 10$ nm at 480°C and remains constant up to 630°C when the size increases rapidly [4]. Also the volume ratio of crystalline to amorphous fraction increases from 0% at 480°C up to 80% at 630°C when further three Fe–B crystal structures are formed.

The present set $Fe_{73.5-x}Si_{13.5}B_9Cu_1Nb_3Mn_x$ ($x = 1, 3 \div 15$) is considered as one of the possible variation of the finemet basic composition.

For the samples the averaged surface composition of as-quenched (a-q) alloys and after annealing (a) was determined at room temperature T_0 by EDX. The results are reasonably well correlated with nominal composition of the glasses except for samples with high Mn content. Since B was not detected, the composition was scaled to Fe nominal atomic content.

The measured Mössbauer spectra of a-q alloys at T_0 are typical of the amorphous structure, with broad line widths caused by hyperfine parameters distribution related to many nonequivalent iron sites. The samples became less and less ferromagnetic as x increases. The spectra were analysed by fitting sextets with distribution of hyperfine field H_{hf} associated with distribution of nonequivalent Fe-sites. The average $\langle H_{\text{hf}} \rangle$ and the average centreshift $\langle CS \rangle$ are shown in Fig. 1a as functions of Mn content x. The $\langle H_{\text{hf}} \rangle$ decreases and asymptotically tends to $\langle H_{\text{hf}} \rangle = 0$ at $x \approx 17$, whereas $\langle CS \rangle$ remains nearly constant.

Also distributions of H_{hf} regularly change as functions of Mn content x, as is shown in Fig. 1b. We can resolve, and draw in Fig. 1a, a strong-field component (H_{H}) and a weak-field contribution (H_{L}) which becomes dominant at large x. For unspecified reason the $x = 13$ distribution breaks slightly the regularity. Structure of the H_{hf} distributions suggests magnetic inhomogeneity of the structurally amorphous initial phase. The H_{L} may be attributed to more diluted, amorphous
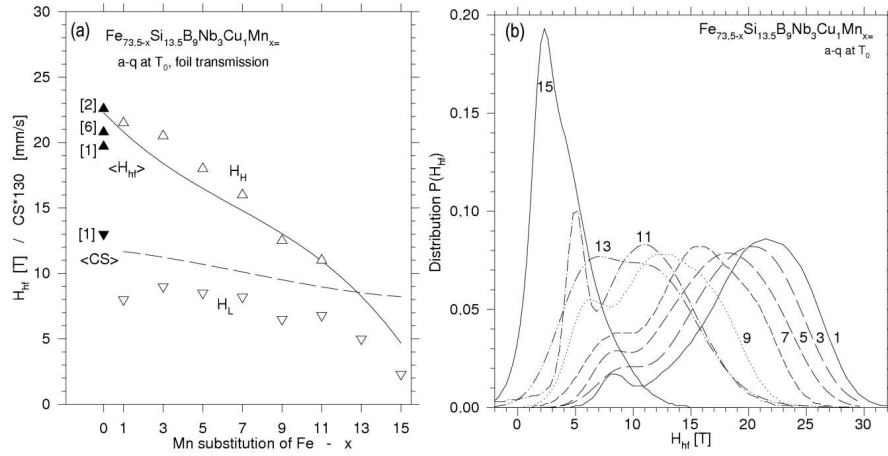
Fig. 1. (a) The average hyperfine fields $\langle H_{hf} \rangle$ (solid line) and centre shifts $\langle CS \rangle$ (dashes). High (H_H) and low (H_L) fields. The solid symbols are the reference data points. (b) The distribution of H_{hf} as functions of x for a-q samples at T_0.

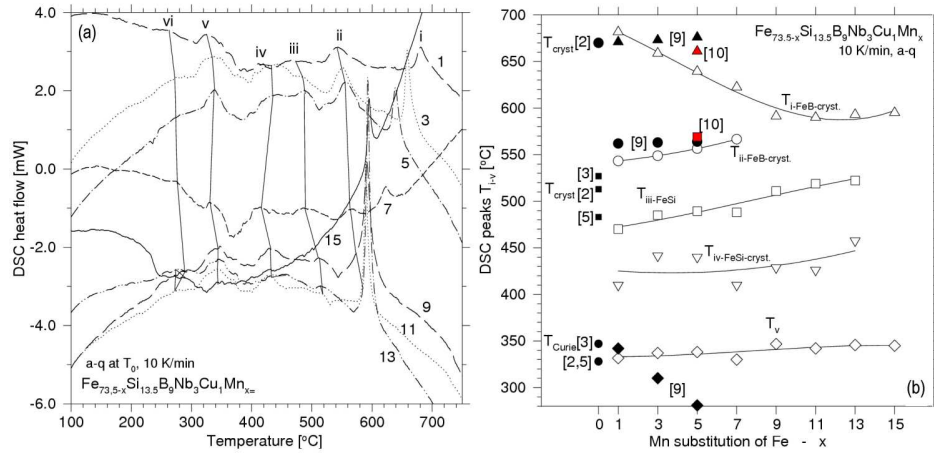Fe solution. The H_H component may be considered as precursor of the crystalline fractions created in annealing.

Fig. 2. (a) DSC temperature scans with resolved peaks marked by i÷v. (b) The peak positions as functions of x (open symbols) with the reference data points (filled).

The DSC scans, at the 10 K/min heating rate, were performed in order to resolve phase transformations regions, Fig. 2a. More or less precisely we can define five (i ÷ v) characteristic exothermic peaks in the heat flow, indicating phase transformations. In consequence, Fig. 2b presents for all x the peak positions $T_{i÷v}$ for the corresponding enthalpy change. Experimental points are supplemented

with 2-point regression curves. Symbols at $x = 0$ mark T_C and T_{cryst} from [2–4]. • and △ mark T_{cryst} and filled ◇ marks T_C from [9] measured at $x = 1, 3, 5$. Two crystallisation temperatures for $x = 5$ from [10] are shown separately.

4. Conclusions

$Fe_{73.5-x}Si_{13.5}B_9Cu_1Nb_3Mn_{x=1,3 \div 15}$ alloys were studied by means of MS, DSC, XRD, EDX as-quenched and after annealing. Mn doping significantly decreases the Curie temperature of amorphous matrix, but moderately the crystallisation temperatures. The hyperfine field for as-quenched alloys is stronger for small values of x, whereas the centre shift remains nearly independent of x.

References

[1] W. Lefebvre, S. Morin-Grognet, F. Danoix, *J. Magn. Magn. Mater.* **301**, 343 (2006).

[2] T. Szumiata, B. Górka, A. Zorkovská, P. Sovák, *J. Magn. Magn. Mater.* **288**, 37 (2005).

[3] J.Z. Jjang, *J. Magn. Magn. Mater.* **154**, 375 (1996).

[4] Y. Hujsheng, T. Guochao, X. Xiotao, X. Zuxiong, M. Ruzhang, *J. Magn. Magn. Mater.* **138**, 94 (1994).

[5] V.A. Peńa-Rodriguez, E.M. Baggio-Savitovich, A.Y. Takeuchi, F. Garcia, E.C. Passamani, J.M. Borrego, A. Conde, *Hyperfine Interact.* **122**, 1 (1999).

[6] J.M. Borrego, V.A. Peńa-Rodriguez, A. Conde, *Hyperfine Interact.* **110**, 1 (1997).

[7] V. Hong Duong, R. Grossinger, R. Sato Turtelli, Ch. Polak, *J . Magn. Magn. Mater.* **157/8**, 193 (1996).

[8] T. Szumiata, K. Brzózka, M. Gawroński, B. Górka, K. Jezuita, J.S. Blazquez--Gamez, T. Kulik, R. Żuberek, A. Ślawska-Waniewska, J.M. Geneche, *J. Magn. Magn. Mater.* **250**, 83 (2002).

[9] N.D. Tho, N. Chau, S.C. Yu, H.B. Lee, L.A. Tuan, N.Q. Hoa, *J. Magn. Magn. Mater.* **304**, e868 (2006).

[10] C. Gomez-Polo, J.I. Perez-Landazabal, V. Recarte, P. Mendoza-Zelis, Y.F. Li, M. Vazquez, *J. Magn. Magn. Mater.* **290-291**, 1517 (2005).